Journal of Biomechanics 44 (2011) 1158–1163

Contents lists available at ScienceDirect

Journal of Biomechanics

journal homepage: www.elsevier.com/locate/jbiomech
www.JBiomech.com

Measurement of the hyperelastic properties of *ex vivo* brain tissue slices

T. Kaster [a], I. Sack [b], A. Samani [a,c,d,*]

[a] Department of Medical Biophysics, University of Western Ontario, London, Ontario, Canada
[b] Department of Radiology, Charité - Universitätsmedizin Berlin, Campus Mitte, Charitéplatz 1, 10117 Berlin, Germany
[c] Department of Electrical and Computer Engineering, University of Western Ontario, London, Ontario, Canada
[d] Imaging Research Laboratories, Robarts Research Institute, London, Ontario, Canada

ARTICLE INFO

Article history:
Accepted 18 January 2011

Keywords:
Finite element method
Surgical simulation
Brain mechanical properties
Hyperelastic modeling
Elastography

ABSTRACT

The elastic and hyperelastic properties of brain tissue are of interest to the medical research community as there are several applications where accurate characterization of these properties is crucial for an accurate outcome. The linear response is applicable to brain elastography, while the non-linear response is of interest for surgical simulation programs. Because of the biological differences between gray and white matter, it is reasonable to expect a difference in their mechanical properties. The goal of this work is to characterize the elastic and hyperelastic properties of the brain gray and white matter. In this method, force–displacement data of these tissues were acquired from 25 different brain samples using an indentation apparatus. These data were processed with an inverse problem algorithm using finite element method as the forward problem solver. Young's modulus and the hyperelastic parameters corresponding to the commonly used Polynomial, Yeoh, Arruda–Boyce, and Ogden models were obtained. The parameters characterizing the linear and non-linear mechanical behavior of gray and white matters were found to be significantly different. Young's modulus was 1787 ± 186 and 1195 ± 157 Pa for white matter and gray matter, respectively. Among hyperelastic models, due to its accuracy, fewer parameters and shorter computational time requirements, Yeoh model was found to be the most suitable. Due to the significant differences between the linear and non-linear tissue response, we conclude that incorporating these differences into brain biomechanical models is necessary to increase accuracy.

1. Introduction

The elastic and hyperelastic properties of brain tissues are of interest to the medical research community as there are several applications where accurate characterization of these properties is crucial for an accurate result. These applications include *in silico* brain models used for surgery or injury simulation (King et al., 1995; Zhang et al., 2001; Zhang et al., 2004). Surgical simulators offer many exciting benefits to both medical teaching institutes as well as neurosurgery residents. They allow residents to train on their own schedule in addition to allowing trainers to review residents' practice sessions before progressing to real surgery (Liu et al., 2003). Simulation models often contain detailed anatomical description but lack accurate validated descriptions of the mechanical properties, and often assume gray and white matter are indistinguishable (Hansen and Larsen, 1998; Miller et al., 2000). Because of the lack of validated tissue properties, the realistic haptic sense of these models may be limited.

Elastography is a method of non-invasively imaging the mechanical properties of body tissues (Ophir et al., 1991). Elastography of the brain combines low-frequency shear waves for remotely stimulating brain tissue through the skull with motion-sensitive magnetic resonance imaging (Muthupillai et al., 1995). This magnetic resonance elastography (MRE) method has been used for studying the linear elastic properties of cerebral tissue (Green et al., 2008; Hamhaber et al., 2007; Klatt et al., 2007; Kruse et al., 2008; Sack et al., 2008; Vappou et al., 2007). Although MRE is capable of investigating the non-linear elastic properties of brain tissue (Sack et al., 2004), the literature lacks *in vivo* studies of brain non-linear MRE. However, since surgical interventions and brain injury impose larger strains, it is important to characterize the non-linear response of cerebral tissues to establish realistic brain models. To further improve the accuracy of such models, it is necessary to distinguish between the biomechanical properties of different tissue types in the brain and elucidate corresponding parameters experimentally. So far, attempts have been made of using *in vivo* MRE for differentiating between gray and white matter; however, contradicting results have been reported (Green et al., 2008; Kruse et al., 2008).

Therefore, this study aims to reveal the elastic properties of gray and white matter and to thoroughly characterize their non-linear elastic properties using *ex vivo* porcine brain slices. The objective of this research is to provide accurate linear elastic and hyperelastic properties of brain gray and white matter that can be

* Corresponding author at: Department of Medical Biophysics, University of Western Ontario, London, Ont., Canada. Tel.: +1 519 661 2111 × 82723.
E-mail address: asamani@uwo.ca (A. Samani).

0021-9290/$ - see front matter © 2011 Elsevier Ltd. All rights reserved.
doi:10.1016/j.jbiomech.2011.01.019

incorporated in brain biomechanical models. Although brain tissue is known to exhibit viscoelastic behaviour, the elastic and hyperelastic properties provide a reasonable estimate of the mechanical properties, especially when the loading rate is low. Applications such as brain surgical simulation and low frequency elastography can benefit from this research.

In the next section, theory of hyperelastic models used in this research will be presented followed by methods, which describe the experimental and data processing approach. The results section presents the measured elastic and hyperelastic properties of brain tissues. Finally, significance of the obtained results and future directions will be presented in the last section.

2. Theory

2.1. Hyperelastic models

This work involves four strain energy models commonly used in biological tissue modeling. The first of these is the Polynomial strain energy function, which is defined as follows:

$$U=\sum_{i+j=1}^{N} C_{ij}(I_1-3)^i(I_2-3)^j+\sum_{i=1}^{N}\frac{1}{D_i}(J_{el}-1)^{2i} \quad (1)$$

where C_{ij} are the parameters of interest that have the units of force per unit area, I_1 and I_2 are strain invariants, J_{el} is the elastic volume strain, and D_i is a compressibility coefficient that tends to zero for incompressible tissues such as brain tissues. In this work, we used a second-order Polynomial strain energy function where $N=2$, which results in five parameters to solve for.

The Yeoh model is a modified form of the $N=3$ Polynomial model where the strain energy function is independent of I_2. This leads to the form

$$U=\sum_{i=1}^{3} C_{i0}(I_1-3)^i+\sum_{i=1}^{N}\frac{1}{D_i}(J_{el}-1)^{2i} \quad (2)$$

where C_{i0}, I_1, I_2, J_{el}, and D_i have the same meanings as in Eq. (1). This formulation results in three parameters.

The Arruda–Boyce model is only dependent on the first strain invariant and is sometimes referred to as the eight chain model. The strain energy function of this model is

$$U=\mu\sum_{i=1}^{5}\frac{C_i}{\lambda^{2i-2}}(I_1^i-3^i)+\frac{1}{D}\left(\frac{{J_{el}}^2-1}{2}-\ln(J_{el})\right) \quad (3)$$

where $C_1=1/2$, $C_2=1/20$, $C_3=11/1050$, $C_4=19/7000$, $C_5=519/673750$. λ is the locking stretch ratio: the stretch where the stress begins to dramatically rise, and μ is the initial shear modulus (Liu et al., 2004). λ and μ are the parameters to be measured.

The Ogden model strain energy equation is directly dependent on the stretches as follows:

$$U=\sum_{i=1}^{N}\frac{2\mu_i}{\alpha_i^2}(\lambda_1^{-\alpha_i}+\lambda_2^{-\alpha_i}+\lambda_3^{-\alpha_i}-3)+\sum_{i=1}^{N}\frac{1}{D_i}(J_{el}-1)^{2i} \quad (4)$$

where α_i are non-dimensional coefficients and λ_i are the deviatoric stretches. For the purposes of this work it was decided to use an Ogden model with an order of one to reduce the number of unknown variables to two: μ the initial shear modulus, and α_1.

3. Methods

3.1. Indentation test apparatus

Very low frequency indentation was used to stimulate tissue samples and measure their static stiffness properties. To accomplish this, the apparatus described in Samani et al. (2003) was used. Fig. 1 is a pictorial representation of the apparatus, which consists of a linear servo actuator, controller, and load cell. We used a 1.5 mm diameter plane-ended indenter for tissue loading. This small size leads to stress propagation through only a small tissue volume around the indenter, hence properly dealing with tissue inhomogeneity. Five sinusoidal loading cycles with 0.1 Hz frequency were applied to each sample. While the amplitude of indentation was 1.5 mm, which translates into 15–20% average strain for 10 mm thick slices, indentation stress concentration leads to much higher strains around the indentation region. This ensures sufficiently large loading for probing the tissues' hyperelastic properties.

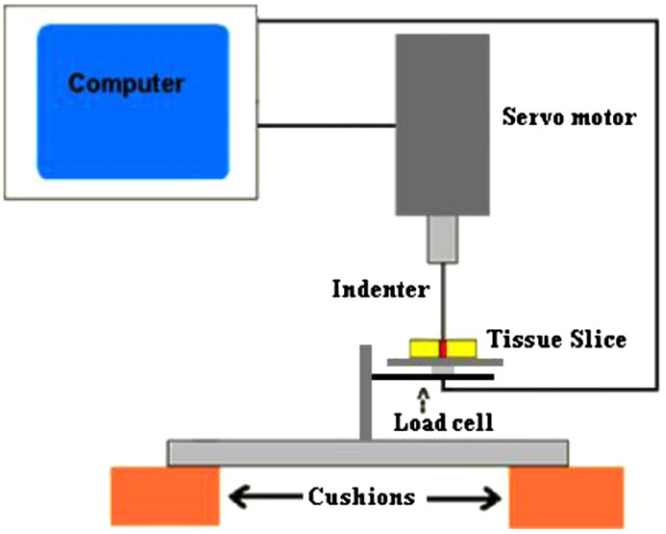

Fig. 1. Schematic of tissue slice elastic and hyperelastic parameters measurement system. It consists of a servo motor for programmed indentation profile and a load cell system for force measurement.

3.2. Tissue slice preparation and measurement protocol

Porcine brain tissue was acquired from a slaughterhouse and tested within 48 h, which was consistent with previous works (Shuck and Advani, 1972; Donnelly and Medige, 1997; Darvish and Crandall, 2001; Nicolle et al., 2004). As soon as the tissue was acquired, it was refrigerated at 4 °C in a saline solution until the experiment where it was warmed to room temperature and cut into 10 mm thick slices. A smooth, homogenous area of white or gray matter was selected for indentation and marked to identify the indentation area.

Before indentation, the slice thickness at the indentation area was measured with digital calipers. This thickness was later used to generate the 3D FE mesh. Thickness measurement was also conducted at randomly selected points across each tissue specimen to ensure thickness variability was not significant. For testing each tissue type, sufficiently large areas were selected with a minimum size of 10D diameter circle where D is the indenter's diameter. For loading, the indenter was manually positioned such that the indenter's end was almost in contact with the marked indentation area selected at its center. To establish full contact with the indenter, the tissue was preloaded with a force of 0.1 g. The machine performed a minimum of 5 cycles of sinusoidal indentation preceded by 20 preconditioning cycles with the same amplitude. The force–displacement data were acquired for offline analysis. To determine whether the indentation process damaged the tissue, a tissue integrity assessment was performed, which involved indenting the tissue at 0.5 mm, then at 1.5 mm, then once more at 0.5 mm. The initial slopes of the indentation experiments at 0.5 mm were compared to determine if there were any significant differences before and after the indentation experiment.

Among the five force–displacement cycles data, the second cycle was processed for two reasons. First, Samani and Plewes (2007) observed that the first cycle was usually less smooth than the subsequent cycles, which precluded using the first cycle. They also noticed that there was a small but incrementally progressing plastic deformation in the tissue throughout the loading cycles. This could be due to contact stress concentration or tissue dehydration at the indenter–tissue contact area. This implies that the second cycle is the most appropriate for further analysis.

3.3. Tissue slice finite element mesh generation

To calculate the hyperelastic parameters, tissue specimen's FE model was created. This involved creating a homogenous cylindrical mesh of radius 10r where r is the radius of the indenter, which was 0.75 mm. The 10r radius was chosen

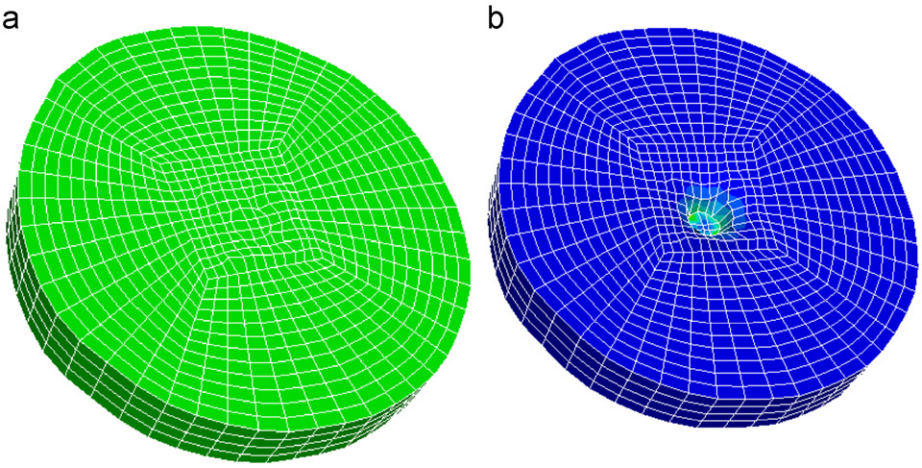

Fig. 2. Typical FE mesh of brain tissue slices. (a) Undeformed FE mesh and (b) deformed FE mesh illustrating indentation simulation.

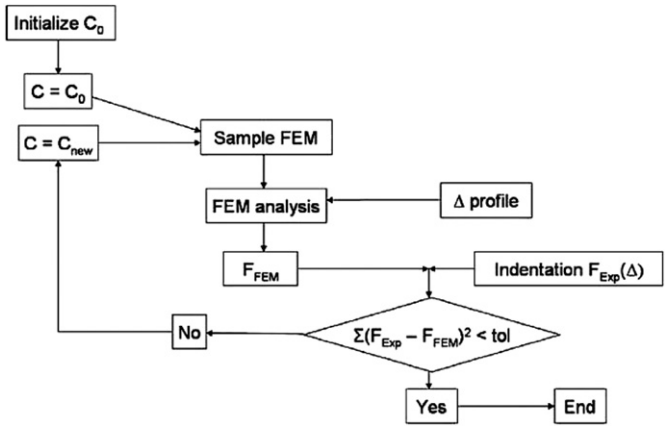

Fig. 3. Flow chart of the optimization procedure used to calculate brain tissue hyperelastic parameters.

because numerical FE experiments indicated that there was insignificant vertical and in-plane displacements and stresses at the model's edges. The mesh consisted of 8-noded hexahedral elements. To include tissue incompressibility hybrid elements were used. Fig. 2 illustrates the results of the FE meshing process, which was created using a transfinite interpolation technique. Details of this meshing technique are given in O'Hagan and Samani (2008). The mesh in this work contained 8064 elements. Finite element mesh convergence study was conducted and we concluded that increasing the number of elements beyond the chosen level had very little impact on the constructed hyperelastic parameters. The boundary conditions were set such that the bottom nodes of the mesh are fixed in the z-direction along the indentation, but free to move in the *x-y* plane. Given the localized loading in indentation, it is expected that uncertainty in this sliding boundary condition does not have a significant effect on the indentation response. The indentation loading of the flat ended indenter was set using prescribed boundary conditions of -1.5 mm in the z-direction.

3.4. Young's modulus calculation

To determine Young's modulus (E), the method described in Samani et al. (2003) was used. This method is based on the following relationship:

$$E = kS \tag{5}$$

where S is the slope of the force–displacement data, and κ is a constant, which depends only on the boundary conditions and indenter geometry. Here, κ is obtained by inputting an arbitrary elastic modulus (E_{arb}) into a linear elastic FE model of the tissue slice. The software simulates indentation, which results in a set of force–displacement data from which the slope can be calculated (S_{Cal}). κ is calculated by substituting S_{Cal} and E_{arb} into Eq. (5). Multiplying the calculated constant by the experimental tissue response slope (S_{meas}) provides E. For calculating S_{meas}, only the initial 0.25 mm indentation was considered to avoid non-linear behavior.

3.5. Optimization algorithm for hyperelastic parameters calculation

To determine the hyperelastic parameters, the algorithm summarized in Fig. 3 was used. This optimization algorithm is a modified version of the algorithm developed by O'Hagan and Samani (2008). This algorithm changes a set of hyperelastic parameters systematically to find the parameter set that yields the best FE force–displacement fit to its measured response. As depicted in Fig. 3, this optimization process is iterative, with the first step being the construction of the tissue specimen's FE mesh. Next, the hyperelastic parameters are initialized to create the FE model, followed by inputting the indentation data and starting FE analysis. From this analysis the reaction forces are output, and the sum of their differences with the experimental forces are calculated. This least squares error is compared to a user-defined tolerance. If the tolerance condition is met, the optimization is terminated. If not, the hyperelastic parameters are updated. To achieve the best accuracy and convergence, two different methods were utilized for updating the parameters depending on the hyperelastic model. For the Yeoh and Polynomial models, we used the slope-variation technique developed by O'Hagan and Samani (2008), whereas for the Ogden and Arruda–Boyce models, we employed the Nelder–Mead method 1965 (Nelder and Mead, 1965). In all cases, the iterative process was terminated when the specified tolerance condition was met, at a maximum of 40 iterations, or when the least-squares error measure displayed no improvement.

To ensure uniqueness of the calculated parameters, the optimization algorithm was performed with various initial estimates. It was found that the final calculated parameters for every model were independent of the initial estimates.

4. Results

The indentation protocol described above was applied to 25 brain samples consisting of 38 white matter and 50 gray matter areas where indentation was performed. Depending on the slice thickness, this resulted in an approximate strain ranging from 15% to 20%; however, FE analysis indicated that the maximum principal strain reaches as much as 70% in the region underneath the indenter. Such strain is quite sufficient for probing the tissues' hyperelastic properties. As seen in Fig. 4, which depicts a typical tissue response, the data display significant non-linearity in the stress–strain response. For each tissue sample, up to three indentation tests were performed on each location, which were averaged into a single value.

For Young's modulus of porcine brain tissue, it was found that white matter had Young's modulus of 1787 ± 186 Pa and gray matter had Young's modulus of 1195 ± 157 Pa. The difference in these values was found to be statistically significant using a two-tailed Student's t-test ($P < 0.001$). Fig. 5 illustrates the results of the integrity assessment performed with 8 different samples. The results fit a straight line fairly well. Using a two-tailed Student's t-test it was found that the initial slope of the 0.5 mm indentation is not significantly different before or after the 1.5 mm

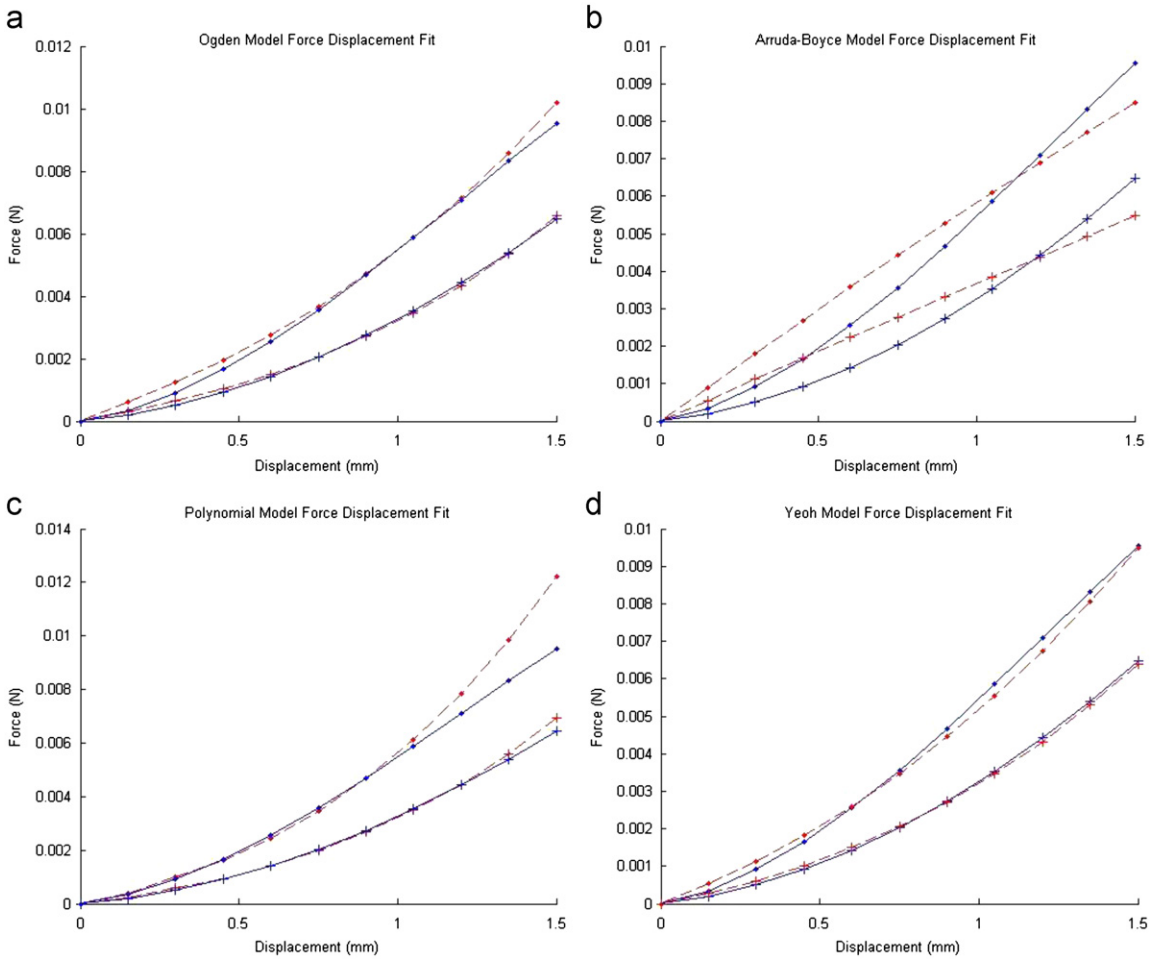

Fig. 4. Typical fit of the strain energy models for gray and white brain tissue. In this figure, each of the four models was fit to the same set of experimental data from white ("•") and gray ("+") matter. The four models were the (a) Ogden, (b) Arruda–Boyce, (c) Polynomial, and (d) Yeoh models. The dashed line is the FE results and solid line is the experimental curve.

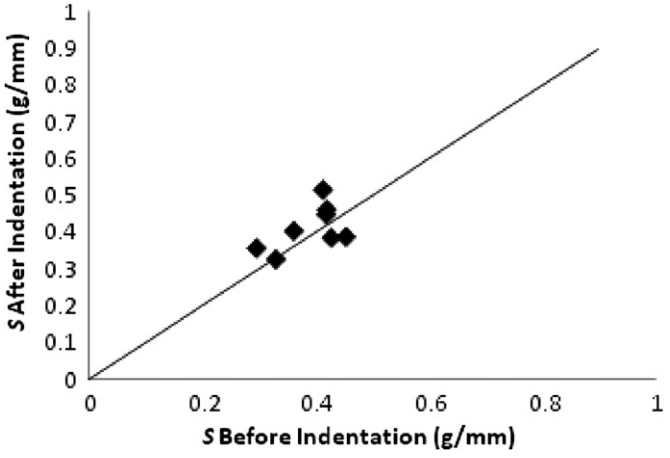

Fig. 5. Tissue integrity assessment. Force–displacement slope (S) calculated before indentation applied (horizontal axis) and after 1.5 mm indentation was applied (vertical axis).

indentation ($P > 0.46$). The results of the indentation experiments for porcine brain are summarized in Table 1. In terms of the difference between white and gray matter, it was found that the μ-parameter of the Ogden and Arruda–Boyce models, C_{10} and C_{20} parameters of the Yeoh model, and C_{10}, C_{01}, C_{11}, C_{20} C_{02} parameters of the second-order Polynomial model were all

Table 1
Results of indentation experiments of porcine white and gray matter specimens. The units for all the parameters – excluding the unitless Arruda–Boyce locking stretch ratio and Ogden α-parameter – are in Pascals (N/m^2).

Strain energy model	Parameter	White tissue	Gray tissue	P-value
Arruda–Boyce	μ	624 ± 144	422 ± 87	1.25E−16
	λ	1.60 ± 0.22	1.57 ± 0.25	0.617
Ogden	μ	624 ± 144	422 ± 87	1.25E−16
	α	17.9 ± 4.3	17.8 ± 4.26	0.810
Yeoh	C_{10}	287 ± 69	185 ± 40	4.26E−17
	C_{20}	1002 ± 441	601 ± 251	4.33E−9
	C_{30}	0.012 ± 0.006	0.010 ± 0.004	0.087
Polynomial	C_{10}	101 ± 26	7.16 ± 14.30	1.10E−12
	C_{01}	101 ± 26	7.16 ± 14.30	1.10E−12
	C_{11}	2410 ± 1070	1320 ± 479	1.60E−11
	C_{20}	16.3 ± 16.8	4.59 ± 2.55	1.05E−7
	C_{02}	16.3 ± 16.8	4.59 ± 2.55	1.05E−7

significantly different ($P < 0.001$). We were unable to conclude that the α-parameter of the Ogden model ($P > 0.810$), λ of the Arruda–Boyce model ($P > 0.617$) or C_{30} of the Yeoh model ($P > 0.087$) were significantly different between white and gray matter.

The models are compared in Table 2. It was found that the best fit of the simulated to experimental data corresponds to the Yeoh and Polynomial models which were approximately equal. The second best corresponds to the Ogden model followed by the

Table 2
Summary of the results from the different strain energy models. The mean error represents the average errors between the actual and simulated indentation forces during indentation.

Model	Mean error (%)	Mean number of iterations	Number of parameters
Yeoh	9.71	5.85	3
Polynomial	8.72	3.58	5
Ogden	11.45	30.17	2
Arruda–Boyce	38.25	9.52	2

Arruda–Boyce model. The Ogden and Arruda–Boyce both required more iterations than the Yeoh and Polynomial model.

5. Discussion and conclusions

This article presents a technique for measuring Young's modulus and hyperelastic parameters of brain tissues including white matter and gray matter. The calculated Young's moduli appear to validate the assumption made in several MRE studies that gray and white matters have significantly different mechanical properties (Green et al., 2008; Kruse et al., 2008). However, contrary to Green et al. (2008), we observed a higher stiffness in white matter than in gray matter. Kruse et al. (2008) also found a higher stiffness of white matter compared to gray matter, however, with more than an order of magnitude higher values compared to our results. This huge difference in absolute values can be attributed neither to the higher dynamic range examined in MRE nor to the differences between conditions in living brain and *ex vivo* tissue samples. Vappou et al. (2007) have compared MRE with rotational rheometry and reported a good agreement between both methods by extrapolating from very low frequencies (0.1 Hz) to the frequency range of MRE (several tens of Hertz). Investigating white matter samples of porcine brain at 0.1 Hz, they found an approximately 1.5-fold lower shear modulus than measured by our indentation technique. At 100 Hz their data indicated 1.1 kPa value. *In vivo* MRE on human brain revealed shear modulus values from 1.2 kPa at 25 Hz (Sack et al., 2008; Wuerfel et al., 2010) to 3.1 kPa at 90 Hz (Green et al., 2008) or – based on a frequency-independent viscoelastic model – 2.1 kPa in healthy volunteers between 18 and 59 years (Wuerfel et al., 2010) and 1.9 kPa including elderly subjects (Sack et al., 2009). The higher Young's modulus observed in living human brain may be attributed to the confining nature of the skull creating a stiffening artifact (Gefen and Margulies, 2004) and inherent differences in the mechanical tissue structure of human and porcine brain (Prange and Margulies, 2002; Nicolle et al., 2004).

Brain tissue hyperelastic parameters corresponding to four hyperelastic models were also measured. Most of these parameters were significantly different for white matter and gray matter tissues. This finding signifies the importance of assigning different mechanical properties for brain tissues in FE computational models. We expect that this finding is equally valid for human brain tissues. While the brain tissue data in this work was based upon a 15–20% average strain, the hyperelastic parameters obtained can still be considered reliable. This is because while only a 15–20% average strain was imposed, the range of strains varied from nearly zero up to 70% beneath the indenter. Furthermore, indentation leads to significant values of all normal and shear stress components. Therefore, the estimated hyperelastic parameters can be regarded as a good representative of brain tissue behavior under various loading modes. Due to the fragile nature of brain tissues, we were concerned that applying large strains could have caused tissue damage. As such, we performed tissue integrity assessment to ascertain that tested samples were not damaged as a result of the procedure. The assessment procedure indicated that the initial slopes of the experiment before and after 1.5 mm indentations were found to not be significantly different. Among the four hyperelastic models we tested we found that the Arruda–Boyce and Ogden models are not favorable because of the large mean error and large number of required iterations. The Polynomial and Yeoh models both reached very good accuracy after a small number of iterations. The Polynomial and Yeoh models led to mean errors of 8.72% and 9.71%, respectively. The small error difference confirms that hyperelasticities of brain tissues have weak dependence on the second strain invariant. Therefore, using the Yeoh model for brain tissues is suitable as it has fewer parameters (3 instead of 5) and leads to better convergence behavior. Also, at larger strains the Polynomial model poorly describes the tissue behaviour, especially the white matter as seen in Fig. 4c.

A limitation of this study is imposed by selecting tissue samples without consideration of white matter fiber alignment. The mechanical anisotropy of white matter was characterized by Prange and Margulies (2002) demonstrating by shear rheometer tests that the shear modulus along the fibers is significantly elevated compared to the perpendicular direction. However, this observation was primarily made inside the corpus callosum while outside this region anisotropy was observed to a much lesser extent. Although we have not used tissue samples from the corpus callosum we cannot exclude influences of white matter fiber alignment and direction effects on our data. A further limitation may arise from the relatively large thickness of gray matter samples which was chosen for consistency purposes. Since our intention was to compare the mechanical behavior of tissue samples from the interior of the brain with cortical areas, consistently 10 mm wide slices were chosen rather than applying anatomically based segmentation. Since the thickness of gray matter is known to range between 2 and 6 mm (Scott et al., 2009) our determined white-to-gray mater ratio of approximately 1.5 could be diluted by white matter tracks within gray matter samples. Another criticism that may be levied against this work is the assumption of tissue homogeneity surrounding the indentation location. However, this is a reasonable assumption for several reasons. The first is that the indentation location was selected based on a visual inspection that confirmed the surrounding area was relatively homogenous. Due to the fact that the indentation test only stimulates tissues locally, the response is mainly influenced by the small tissue region around the indenter. Any tissue inhomogeneities distant from the indentation location will have minimal impact on the measured results. This assumption appears to be borne out by the consistency of the results. For example, the coefficient of variation of white matter in the Ogden model for the two parameters was 23.1% and 24.2%, while for gray matter it was 20.6% and 23.9%. These variations include inter-subject variations, experimental and sampling errors in addition to errors pertaining to tissue inhomogeneity. This implies that measurements made at numerous indentation locations, with different concentrations of gray and white matter did not appear to adversely affect the results. Further research is required to measure brain tissue mechanical properties under dynamic loading. Such properties are necessary to assess brain tissue damage resulting from head impact. Hrapko et al. 2006 and Hrapko et al. 2008 measured the nonlinear viscoelastic properties of porcine tissues. They tested white matter only. To complement this work the proposed indentation technique can be employed to test both white matter and grey matter nonlinear viscoelastic properties and assess their differences. Such investigation is expected to further improve the accuracy of predicting tissue damage resulting from head impact.

Conflict of interest statement

The authors confirm that this manuscript and its corresponding research work involves no conflict of interest.

Acknowledgment

This research was supported under grants from the Natural Sciences and Engineering Research Council of Canada (NSERC).

References

Darvish, K., Crandall, J., 2001. Nonlinear viscoelastic effects in oscillatory shear deformation of brain tissue. Medical Engineering and Physics 23, 633–645.
Donnelly, B., Medige, J., 1997. Shear properties of human brain tissue. Journal of Biomechanical Engineering—Transactions of the American Society of Mechanical Engineers 119, 423–432.
Gefen, A., Margulies, S., 2004. Are in vivo and in situ brain tissues mechanically similar? Journal of Biomechanics 37, 1339–1352.
Green, M., Bilston, L., Sinkus, R., 2008. In vivo brain viscoelastic properties measured by magnetic resonance elastography. Nuclear Magnetic Resonance in Biomedicine 21, 755–764.
Hamhaber, U., Sack, I., Papazoglou, S., Rump, J., Klatt, D., Braun, J., 2007. Three-dimensional analysis of shear wave propagation observed by in vivo magnetic resonance elastography of the brain. Acta Biomaterialia 3, 127–137.
Hansen, K., Larsen, O., 1998. Using region-of-interest based finite element modeling for brain-surgery simulation. Lecture Notes in Computer Science 1496, 305–316.
Hrapko, M., van Dommelen, J.A.W., Peters, G.W.M., Wismans, J.S.H.M., 2006. The mechanical behaviour of brain tissue: large strain response and constitutive modeling. Biorheology 43, 623–636.
Hrapko, M., van Dommelen, J.A.W., Peters, G.W.M., Wismans, J.S.H.M., 2008. Characterisation of the mechanical behavior of brain tissue in compression and shear. Biorheology 45, 663–676.
Klatt, D., Hamhaber, U., Asbach, P., Braun, J., Sack, I., 2007. Noninvasive assessment of the rheological behavior of human internal organs using multifrequency MR elastography: a study of brain and liver viscoelasticity. Physics in Medicine and Biology 52, 7281–7294.
King, A.I., Ruan, J.S., Zhou, C., Hardy, W.N., Khalil, T.B., 1995. Recent advances in biomechanics of brain injury research: A review. Journal of Neurotrauma 12 (4), 651–658.
Kruse, A., Rose, G., Glaser, K., Manduca, A., Felmlee, J., Jack Jr., C., Ehman, R., 2008. Magnetic resonance elastography of the brain. NeuroImage 39, 231–237.
Liu, A., Tendick, F., Cleary, K., Kaufmann, C., 2003. A survey of surgical simulation: applications, technology, and education. Presence: Teleoperators and Virtual Environments 12, 599–614.
Liu, Y., Kerdok, A., Howe, R., 2004. A nonlinear finite element model of soft tissue indentation. Lecture Notes in Computer Science 3078, 67–76.
Miller, K., Chinzei, K., Orssengo, G., Bednarz, P., 2000. Mechanical properties of brain tissue in-vivo: experiment and computer simulation. Journal of Biomechanics 33, 1369–1376.
Muthupillai, R., Lomas, D., Rossman, P., Greenleaf, J., Manduca, A., Ehman, R., 1995. Magnetic resonance elastography by direct visualization of acoustic strain waves. Science 269, 1854–1857.
Nelder, J., Mead, R., 1965. A simplex method for function minimization. Computer Journal 7, 308–313.
Nicolle, S., Lounis, M., Willinger, R., 2004. Shear properties of brain tissue over a frequency range relevant for automotive impact situations: new experimental results. Stapp Car Crash Journal 48, 239–258.
O'Hagan, J., Samani, A., 2008. Measurement of the hyperelastic properties of tissue slices with tumour inclusion. Physics in Medicine and Biology 53, 7087–7106.
Ophir, J., Cespedes, I., Ponnekanti, H., Yazdi, Y., Li, X., 1991. A quantitative method for imaging the elasticity of biological tissues. Ultrasonic Imaging 13, 111–134.
Prange, M., Margulies, S., 2002. Regional, directional, and age-dependent properties of the brain undergoing large deformation. Journal of Biomechanical Engineering—Transactions of the American Society of Mechanical Engineers 124, 244–252.
Sack, I., Beierbach, B., Hamhaber, U., Klatt, D., Braun, J., 2008. Non-invasive measurement of brain viscoelasticity using magnetic resonance elastography. NMR in Biomedicine 21, 265–271.
Sack, I., Beierback, B., Wuerfel, J., Klatt, D., Hamhaber, U., Papazoglou, S., Martus, P., Braun, J., 2009. The impact of aging and gender on brain viscoelasticity. NeuroImage 46, 652–657.
Sack, I., McGowan, C., Samani, A., Luginbuhl, C., Oakden, W., Plewes, D., 2004. Observation of nonlinear shear wave propagation using magnetic resonance elastography. Magnetic Resonance in Medicine 52, 842–850.
Samani, A., Bishop, J., Luginbuhl, C., Plewes, D., 2003. Measuring the elastic modulus of ex vivo small breast tissue samples. Physics in Medicine and Biology 48, 2183–2198.
Samani, A., Plewes, D., 2007. An inverse problem solution for measuring the elastic modulus of intact ex vivo breast tissue tumours. Physics in Medicine and Biology 52, 1247–1260.
Scott, M., Bromiley, P., Thacker, N., Hutchinson, C., Jackson, A., 2009. A fast, model-independent method for cerebral cortical thickness estimation using MRI. Medical Image Analysis 13, 269–285.
Shuck, L., Advani, S., 1972. Rheological response of human brain tissue in shear. Journal of Basic Engineering 94, 905–911.
Vappou, J., Breton, E., Choquet, P., Goetz, C., Willinger, R., Constantinesco, A., 2007. Magnetic resonance elastography compared with rotational rheometry for in vitro brain tissue viscoelasticity measurement. Magnetic Resonance Materials in Physics, Biology and Medicine 20, 273–278.
Wuerfel, J., Paul, F., Beierbach, B., Hamhaber, U., Klatt, D., Papazoglou, S., Zipp, F., Martus, P., Braun, J., Sack, I., 2010. MR-elastography reveals degradation of tissue integrity in multiple sclerosis. NeuroImage 49, 2520–2525.
Zhang, L. Yang, K. King, A., 2001. Comparison of brain responses between frontal and lateral impacts by Finite Element modeling. Journal of Neurotrauma 18, 21-30.
Zhang, L., Yang, K., King, A., 2004. A proposed injury threshold for mild traumatic brain injury. Journal of Biomechanical Engineering 126, 226–237.